

# Research on Fault Location Method Based on Nonlinear Impedance Model

Ruiying Liu<sup>1</sup>, Zhongjian Kang<sup>1</sup>, and Yanyan Feng<sup>2</sup>

<sup>1</sup> College of Information and Control Engineering, China University of Petroleum, Qingdao 266580, China

<sup>2</sup> Zaozhuang Power Supply Bureau, Zaozhuang 277000, China

Email: {18266632686, kangzjzh}@163.com; 919630086@qq.com

**Abstract**—In modeling and location analysis, most traditional fault location methods do not consider about the existence of practical nonlinear model in distribution network, such as the nonlinearity of load and grounding resistor. Hence, the adopted model can't express the practical network, and the location results will lose practical meaning. Aiming at solving the question above, this paper proposes a fault area location method for distribution network with Distributed Generation (DG) which takes account of the nonlinearity; the load adopts quadric polynomial model; the grounding resistor adopts the experience formula model; the nonlinear equation constructed by nodal voltage equation will be solved out through quasi-newton algorithm, then the fault area can be located according to the definition of fault feature value. The simulation results in 10 kV distribution network model of the SINPOPEC West-Northern oil field suggest the validity of the proposed fault location method.

**Index Terms**—Distributed Generation (DG), fault area location, nonlinear model, quasi-newton algorithm

## I. INTRODUCTION

Fault location has always been one of important hot topic in the field of power system [1]. In the distribution network with Distributed Generation (DG), the traditional structure has been substantially changed. As a result, many scholars proposed fault location methods suitable for distribution network with DG [2]-[6]. The article [5] proposed a fault location method based on fault feature matching and differential evolution algorithm for distribution network with DG which can achieve fault area location according to the search for the minimum fault feature value. On the basis of article [5], article [6] improved the method by adopting complex correlation Thevenin equivalent calculation and Strong Tracking Filter (STF). STF can be adopted for real-time extraction of fundamental voltages' and currents' wave phase and amplitude, and fast track the power parameters' mutation. The method of complex correlation Thevenin equivalent calculation takes the randomness of measurement data and DG into account to overcome measurement error caused by the uncertainty of the measurement data, so that the construction of the DG impedance model is more accurate. However, the fault location theories in article

[5], [6] are all based on superposition principle which can only be suitable for linear systems.

Most common modeling methods for load and grounding resistance respectively adopt constant impedance model and a fixed resistance. In view of the nonlinear factors, this paper proposes a new definition method of fault feature value, adopts quasi-newton algorithm to solve the nonlinear calculations based on the establishment of nonlinear three-phase impedance model and nodal voltage equations. The fault area can be judged out by the search for the minimum fault feature value.

## II. THE ESTABLISHMENT OF NONLINEAR THREE-PHASE IMPEDANCE MODEL

The impedance model in distribution network with DG contains the main source, DG, transformer, line, load and the grounding resistance. Each element adopts three-phase asymmetrical impedance model in this paper. Among them, the modeling methods of main source, DG, transformer and line are not repeated here, which refer to the article [5]. Then the modeling methods of nonlinear load and the grounding resistance are shown below.

### A. Three-Phase Nonlinear Load Impedance Model

Load model which is often adopted in the power system analysis and calculation is the physical simulation and mathematical description of the load characteristic. According to the characteristic of the load, load model can be divided into static model and dynamic model. This paper adopts the static load model.

Quadratic multinomial representation is a common way to represent static load voltage model [7] which is shown as (1).

$$\begin{aligned} P &= P_N \left[ a_p (U/U_N)^2 + b_p (U/U_N) + c_p \right] \\ Q &= Q_N \left[ a_q (U/U_N)^2 + b_q (U/U_N) + c_q \right] \end{aligned} \quad (1)$$

here,  $U_N$ ,  $P_N$  and  $Q_N$  are respectively rated voltage, active power and reactive power of load;  $a_p, b_p, c_p$  are coefficients of the active power expression, while  $a_q, b_q, c_q$  are coefficients of the reactive power expression. The sums of these coefficients are respectively equal to 1 as (2).

$$\begin{aligned} a_p + b_p + c_p &= 1 \\ a_q + b_q + c_q &= 1 \end{aligned} \quad (2)$$

Manuscript received June 5, 2015; revised November 16, 2015.

Project Supported by National Natural Science Foundation of China (61271001) and the Fundamental Research Funds for the Central Universities of China under Grant No. 14CX05039A.

doi:10.12720/jcm.10.11.903-909

From (1), the active and reactive power of load are respectively composed of three parts which include constant resistance load which is proportional to the square of voltage, constant current load which is proportional to voltage and constant power load.

The impedance of this load model can be calculated through the power expression of load which is given by (3).

$$\begin{aligned}
 Y_{LD,j} &= \frac{P_i - jQ_i}{|U_i|^2} \\
 &= P_{iN} [a_p/U_N^2 + b_p/U_N + c_p/U_i^2] - jQ_{iN} [a_q/U_N^2 + b_q/U_N + c_q/U_i^2] \Omega^{-1} \\
 &= \frac{a_p P_{iN} - j a_q Q_{iN}}{U_N^2} + \frac{b_p P_{iN} - j b_q Q_{iN}}{U_N} + \frac{c_p P_{iN} - j c_q Q_{iN}}{U_i^2} \Omega^{-1} \\
 &= Y_{LD,j}(U_i) \Omega^{-1}
 \end{aligned} \tag{3}$$

here,  $i=a,b,c$ ;  $U_i$ ,  $P_i$  and  $Q_i$  are respectively  $i$ -phase rated voltage, active power and reactive power of load.  $Y_{LD}$  calculated by (3) changes with  $U$  as  $P$  and  $Q$  are both functions of  $U$ .

The nonlinear parts of load is firstly processed as following for reducing the complexity and calculation time bringing by nonlinear expressions of load. The quadratic multinomial load model can be equivalent to parallel connection of constant impedance load, constant current load and constant power load.

The voltage and current vector of load can be read from the measurement equipment and respectively recorded as  $\dot{V}_L, \dot{I}_L$ ; ZIP load could be equivalent to the parallel connection of constant impedance and variable current source.

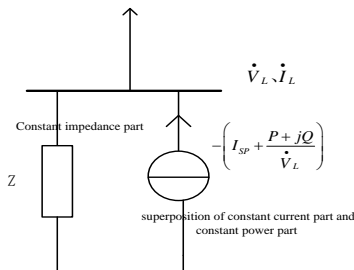


Fig. 1. Equivalent diagram of load model.

Here, the power of the constant impedance load is  $P = P_N [a_p (U/U_N)^2]$ ,  $Q = Q_N [a_q (U/U_N)^2]$ , therefore the constant impedance can be calculated as  $Z = R + jX = \frac{V_0^2}{a_p P_0} + j \frac{V_0^2}{a_q Q_0}$ .

As shown in Fig. 1, when establishing the system's three phase admittance matrix, only  $Z^{-1}$  will be taken to self-admittance of the load, while  $-(I_{sp} + (P + jQ)/\dot{V}_L)$  will be regarded as injection current and taken to injection current vector of the system.

### B. Three Phase Nonlinear Impedance Model of the Ground Resistance

Arc grounding resistance value is a nonlinear function of fault current. Its impedance model is derived in article [8].

$$R(I_{fi}) = \left( \frac{855.3L_i}{I_{fi}} + \frac{4501.6L_i}{I_{fi}^2} \right) \tag{4}$$

here,  $i=a,b,c$  phase;  $L_i$  is the arc length when an arc fault occurs at phase  $i$ ;  $I_{fi}$  is the fault current of phase  $i$ .

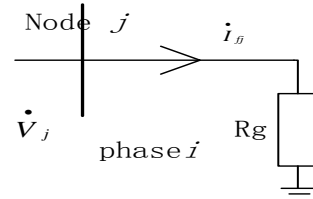


Fig. 2. Analysis diagram of fault node in fault.

In Fig. 2, assuming that an arc fault occurs at  $i$  phase of the  $j^{th}$  node,  $\dot{V}_j, \dot{I}_{fi}, R_g$  and  $L_i$  are respectively voltage, current, grounding resistance and arc length in fault, the relationship between node voltage and grounding resistance of the fault phase is derived as (5)-(7).

$$R_g = \frac{\dot{V}_j}{\dot{I}_{fi}} = R(I_{fi}) \tag{5}$$

$$\dot{I}_{fi} = \frac{4501.6L_i}{\dot{V}_j - 855.3L_i} \tag{6}$$

$$R(\dot{V}_j) = \frac{(\dot{V}_j - 855.3L_i)\dot{V}_j}{4501.6L_i} \tag{7}$$

### C. The Formation of System's Three-Phase Admittance Matrix

According to the network structure and the parameters of each model, the three phase node admittance matrix of a power system with  $n$  nodes is shown below.

$$Y_{abc} = \begin{bmatrix} Y_{11} & Y_{12} & \cdots & Y_{1n} \\ Y_{21} & Y_{22} & \cdots & Y_{2n} \\ \vdots & \vdots & \vdots & \vdots \\ Y_{n1} & Y_{n2} & \cdots & Y_{nn} \end{bmatrix}_{3n \times 3n} \tag{8}$$

here,  $Y_{nn}$  is the self-impedance of the  $n^{th}$  node;  $Y_{nm}$  is the mutual impedance between the  $n^{th}$  node and the  $m^{th}$  node.

The node impedance matrix and node admittance matrix are mutually inverse matrix. Thus, the three-phase impedance model has been established.

## III. FAULT AREA LOCATION METHOD IN DISTRIBUTION NETWORK WITH DG

### A. Fault Feature Extraction

While fault occurs in distribution network with DG, the system still meets the network equations [9] shown as (10).

$$Y^{(f)}V^{(f)} = I^{(f)} \tag{10}$$

here,  $Y^{(f)}$  is the three-phase admittance matrix in fault;  $V^{(f)}$  is the system's node voltage vector in fault;  $I^{(f)}$  is the system's injection current vector in fault which can be obtained by the measuring equipment at sources and loads.

Assuming that  $m$  is the total number of source points which are defined respectively as  $Bus(1), Bus(2) \dots Bus(m)$ , and  $k$  is the total number of load points which are respectively defined as  $Bus(m+1) \dots Bus(m+k)$ ; The arc fault occurs at the  $j^{th}$  node, the voltage and injection current of each power measurement point can be measured synchronously. The measured voltages at each power points pre fault are respectively defined as  $\dot{V}_{BS}(1), \dot{V}_{BS}(2) \dots \dot{V}_{BS}(m)$ , and the measured voltages and currents at each load point in fault are respectively defined as  $\dot{V}_{BS}'(1), \dot{V}_{BS}'(2) \dots \dot{V}_{BS}'(m)$  and  $\dot{I}_{BS}'(1), \dot{I}_{BS}'(2) \dots \dot{I}_{BS}'(m+k)$ .

Three-phase node voltage vector is defined as  $U = [\dot{V}_{BS}(1) \dot{V}_{BS}(2) \dots \dot{V}_{BS}(n)]^T$ , where  $\dot{V}_{BS}(n)$  is the three-phase voltage vector of the  $n^{th}$  node. The current vector of source can be obtained through the source measurements which are defined as  $\dot{I}_s = [\dot{I}_{BS}(1) \dot{I}_{BS}(2) \dots \dot{I}_{BS}(m) \ 0 \ \dots \ 0]^T$ , where  $\dot{I}_{BUS}(m)$  is the three phase current vector of the  $m^{th}$  node. From the analysis in 1.1, the currents of the loads' equivalent injection current source are respectively  $-(\dot{I}_{BS}'(m+1) - \frac{\dot{V}_{BS}'(m+1)}{Z_{load1}}), \dots, -(\dot{I}_{BS}'(m+k) - \frac{\dot{V}_{BS}'(m+k)}{Z_{loadm+k}})$ .

So the loads' equivalent injection current vector is  $\dot{I}_{load} = \left[ 0 \ \dots \ 0 \ -(\dot{I}_{BUS}'(m+1) - \frac{\dot{V}_{BUS}'(m+1)}{Z_{load1}}) \ \dots \ -(\dot{I}_{BUS}'(m+k) - \frac{\dot{V}_{BUS}'(m+k)}{Z_{loadm+k}}) \ 0 \ \dots \ 0 \right]^T$ . Therefore the system's injection current vector in fault can be obtained as  $\dot{I}^{(f)} = \dot{I}_s^{(f)} + \dot{I}_{load}^{(f)}$ .

The admittance matrix in fault needs to be modified by (11) according to the arc resistance which is the nonlinear function of fault voltage while an arc fault occurs at the  $j^{th}$  node (shown as Fig. 3).

$$Y^{(f)}(j, j) = Y(j, j) + R_g^{-1} = Y(j, j) + (R(\dot{V}_j))^{-1} \quad (11)$$

Therefore, the admittance matrix and nodal voltage equations in fault all become nonlinear functions about fault voltages. The problem of obtaining fault voltage becomes the solution of nonlinear equations.

Choose:

$$F(\dot{V}^{(f)}) = Y^{(f)}(\dot{V}^{(f)})\dot{V}^{(f)} - \dot{I}^{(f)} = 0 \quad (12)$$

$\dot{I}^{(f)}$  is the obtained quantity, the node voltages are the variables.

Common algorithms for solving nonlinear equations are simple iteration methods, Newton iteration methods, quasi-Newton iterative methods and intelligent optimization algorithms [10] etc. This paper adopts quasi-newton iterative method introduced in article [11] to obtain node voltage vector in fault  $V^{(f)}$  in view of the complexity and iterations of the algorithms. In theory, the calculated voltage vectors of measuring points are equal to the measured ones.

The definition of fault feature value is as follows:

The error between the calculated fault voltages in the measuring points and the measured ones when the arc

fault occurs is defined as fault feature value. And this fault characteristic value noted as  $E(j)$  by assuming the fault position is at the  $j^{th}$  node is defined as (13). In the actual fault node, the fault feature value is the nearest to 0.

Therefore the fault feature value of the  $j^{th}$  node is:

$$E(j) = \sum_{n=1}^{m+k} \left| \dot{U}_{cal.j}(n) - \dot{U}_{mea}(n) \right| \quad (13)$$

here,  $\dot{U}_{cal.j}(n)$  is the calculated voltage vector of the  $n^{th}$  measurement point by assuming the fault occurs at the  $j^{th}$  node;  $\dot{U}_{mea}(n)$  is the measured voltage of the  $n^{th}$  measurement point.

Assuming the fault node is respectively from the first node until the last node, the assumed fault node is used to form corresponding nonlinear network equations and calculate the corresponding fault feature value. If the assumed fault node is the actual fault node,  $E(j)$  will be the smallest one in all fault feature values. The three minimum of the values will be selected for avoiding misjudgments; the three corresponding nodes respectively named as  $K_1, K_2$  and  $K_3$  are fault associated nodes.

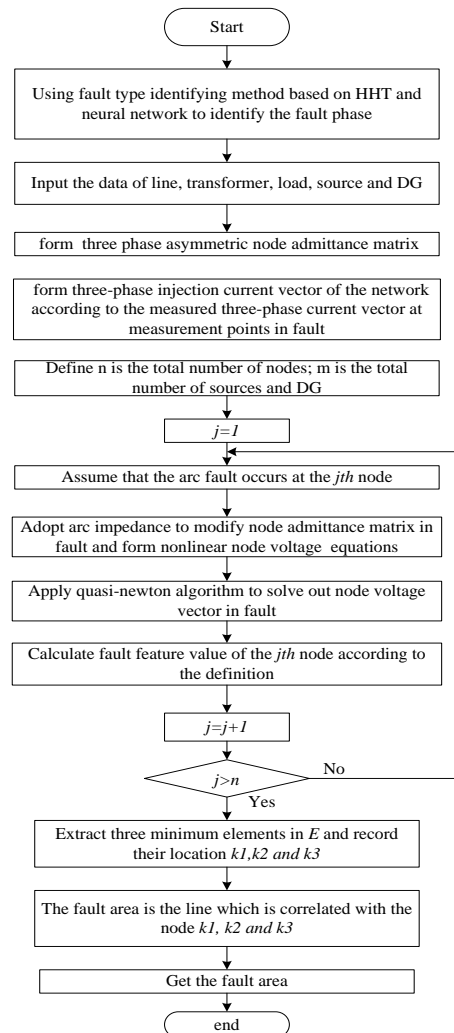


Fig. 3. Fault area location in distribution network with DG.

**B. Implementation of Fault Area Location Method Based on Nonlinear Impedance Model**

The steps of fault area location are:

- 1) Read in the relevant parameters of power supply, lines and load for the establishment of three-phase impedance model;
- 2) Read in three-phase current vector at measurement points in fault to form three-phase injection current vector of the network;
- 3) Build nonlinear equations about node voltages in view of arc nonlinear model by assuming that the fault location is at the  $j^{th}$  node;
- 4) Apply quasi-newton algorithm to solve out node voltage vectors;
- 5) Calculate  $E(j)$  assuming that the fault location is at the  $j^{th}$  node according to the definition introduced above while  $j$  is assumed from the first node to the  $n^{th}$  node, then the calculated fault feature value can be respectively defined as  $E(1), E(2) \dots E(n)$ ;
- 6) Select three minimum of the values for avoiding misjudgments, the three corresponding nodes respectively named as  $K1, K2$  and  $K3$  are fault associated nodes;
- 7) Judge out the lines which are connected with the fault associated nodes as possible fault lines, then confirm the fault area.

According to the electrical network theory, the calculated voltage is equal to the actual voltage at measurement points, that the fault feature value at actual fault point is smallest.

The detailed flow chart of fault area location method in distribution network with DG is shown as Fig. 3.

**IV. SIMULATIONS**

**A. The Simulation Model**

The method proposed in this paper is tested in an actual 10 KV substation AiDing in XinJiang. The distribution network simulation system model is built in Matlab/Simulink, which is shown as Fig. 5. The total length of the lines are 58.2 km, while the first node to the 18<sup>th</sup> node are nodes of the main lines (LGJ-120/20mm<sup>2</sup>), the 19<sup>th</sup> node to the 64<sup>th</sup> node are nodes of branch lines (LGJ-50/8mm<sup>2</sup>). The total load is 3.6 MVA, the DG unit capacity and access point is shown in Table I, all the DG units account for 47% of the total load. The software implementation consists of two parts. The first part is modeling in Simulink; the source and DG adopt three-phase source, the line adopts three-phase PI section line; In Matlab/Simulink environment, there are two types of arc for selection including Cassie arc model and Mayr arc model provided by P.H. Schavemaker, Power Systems Laboratory, Delft University of Technology, the Netherlands. The Cassie arc model is adopted in the simulation model in Fig. 5 (a); the load adopts ZIP model shown in Fig. 5(b). The second part is to programming in MATLAB to implement the calculation of the fault feature value and the selection of the minimum value.

The simulation in Simulink can provide the measured voltage and current signals which can be import into MATLAB for the implementation of the fault location method.

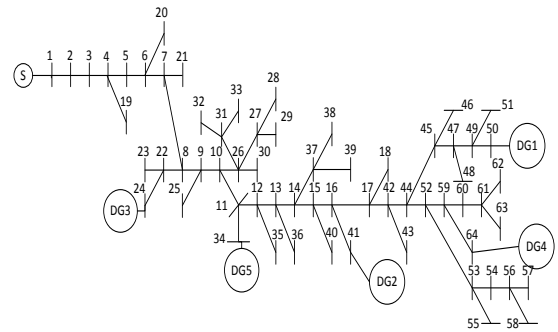
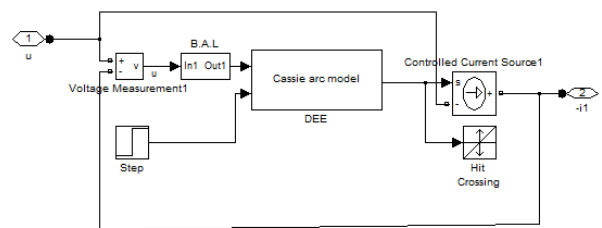
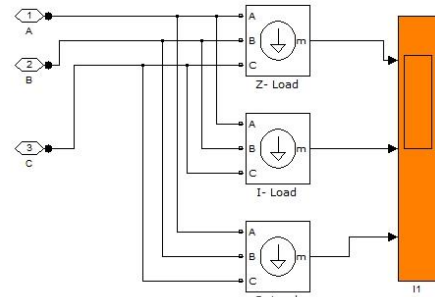


Fig. 4. Topology of the system.



(a) the arc model in SIMULINK library



(b) ZIP load model

Fig. 5. The SIMULINK model of arc and load.

TABLE I: CAPACITY AND ACCESS POINT OF DG UNIT

name	Access point	capacity/ MVA	name	Access point	capacity/ MVA
DG1	50	0.5	DG4	64	0.3
DG2	41	0.2	DG5	34	0.2
DG3	24	0.4			

**B. Fault Area Location Results**

Case1: when a single grounding fault occurs at the second node, the fault feature value in fault can be calculated by the programs through assuming the fault occurs at different nodes. The simulation results are shown in Fig. 6.

From Fig. 6, the three minimum of fault feature value is at the first, second and third node. Also, the feature value of the 19<sup>th</sup> node is less than the surrounding nodes which is because the 19<sup>th</sup> node is connected with the 4<sup>th</sup> node from Fig. 4. The changing rule obeys the introduced theory: the nearer the node is away from fault node, the smaller the fault feature value is.

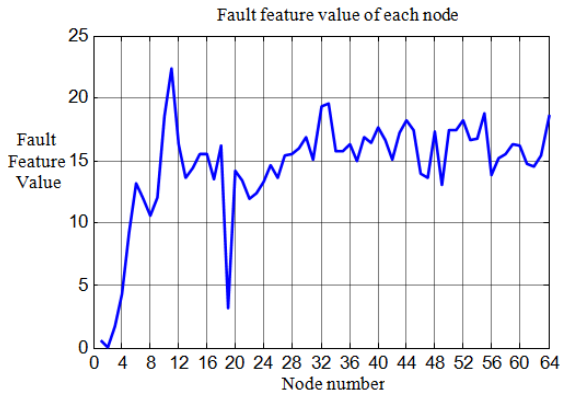


Fig. 6. Fault feature value waveform when single grounding fault occurs at the second node.

The output location result is the lines associated with node 1, 2, 3. Hence the fault area can be located confidently.

Case 2: When a single grounding fault occurs at the 25<sup>th</sup> node, the fault feature value in fault can be calculated by the programs through assuming the fault occurs at different nodes. The simulation results are shown in Fig. 7.

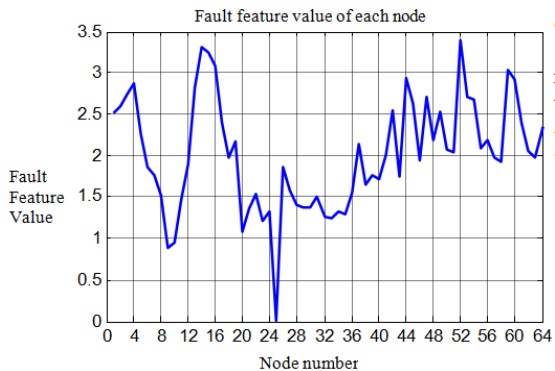


Fig. 7. Fault feature value waveform when single grounding fault occurs at the 25<sup>th</sup> node.

It can be seen from Fig. 4 that the 25<sup>th</sup> node is linked with the 9<sup>th</sup> and 10<sup>th</sup> node. From Fig. 7, the three minimum of fault feature value is at the 25<sup>th</sup>, 9<sup>th</sup> and 10<sup>th</sup> node.

The output location result is the lines associated with the 25<sup>th</sup>, 9<sup>th</sup> and 10<sup>th</sup> node. Hence the fault area can be located confidently.

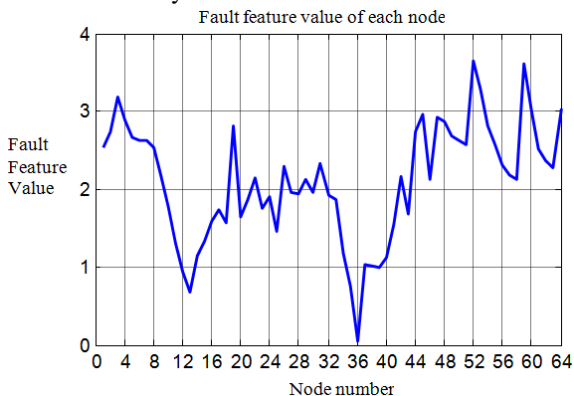


Fig. 8. Fault feature value waveform when two-phase (AB) grounding fault occurs at the 36<sup>th</sup> node

Case 3: When a two-phase arc fault occurs at the 36<sup>th</sup> node, the fault feature value in fault can be calculated by the programs through assuming the fault occurs at different nodes. The simulation results are shown in Fig. 8.

It can be seen from Fig. 4 that the 36<sup>th</sup> node is linked with the 13<sup>th</sup> and 35<sup>th</sup> node. From Fig. 8, the three minimum of fault feature value is at the 13<sup>th</sup>, 35<sup>th</sup> and 36<sup>th</sup> node.

The output location result is the lines associated with node 13, 35, 36. Hence the fault area can be located confidently.

Case 4: When a two-phase arc fault occurs at the 59<sup>th</sup> node, the fault feature value in fault can be calculated by the programs through assuming the fault occurs at different nodes. The simulation results are shown in Fig. 9.

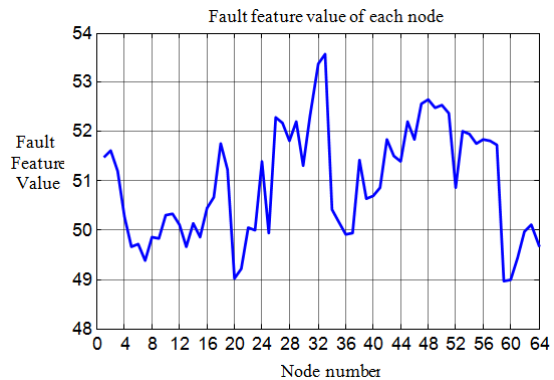


Fig. 9. Fault feature value waveform when three phase grounding fault occurs at the 59<sup>th</sup> node.

It can be seen from Fig. 4 that the 59<sup>th</sup> node is linked with the 60<sup>th</sup> and 20<sup>th</sup> node. From Fig. 9, the three minimum of fault feature value is at the 59<sup>th</sup>, 60<sup>th</sup> and 20<sup>th</sup> node.

The output location result is the lines associated with the 59<sup>th</sup>, 60<sup>th</sup> and 20<sup>th</sup> node. Hence the fault area can be located confidently. The 59<sup>th</sup> node is linked with the 60<sup>th</sup> and 20<sup>th</sup> node from Fig. 5.

As space is limited, simulation results only for distribution network with single phase arc fault are listed in this paper as Table II.

TABLE II: PARTIAL FAULT AREA LOCATION RESULTS

Fault node	Location result	Right or wrong
1	Node 1 , 2, 3	√
5	Node 5 , 6, 4	√
7	Node 21 , 7, 6	√
8	Node 24 , 22, 23	×
10	Node 11 , 10, 26	√
11	Node 11 , 10, 34	√
19	Node 19 , 1, 2	√
20	Node 6 , 20, 7	√
21	Node 21 , 7, 6	√
23	Node 23 , 24, 22	√
24	Node 24 , 23, 22	√
26	Node 27 , 26, 30	√
27	Node 27 , 26, 28	√
28	Node 28 , 27, 29	√

29	Node 29 , 28, 30	√
30	Node 30 , 28, 29	√
32	Node 32 , 31, 33	×
34	Node 34 , 11, 10	√
35	Node 36 , 12, 13	×
37	Node 37 , 38, 39	√
38	Node 38 , 37, 39	√
39	Node 39 , 38, 37	√
40	Node 40 , 15, 14	√
43	Node 43 , 42, 17	√
44	Node 42 , 44, 17	√
45	Node 45 , 46, 47	√
48	Node 47 , 48, 45	√
49	Node 49 , 50, 47	√
50	Node 50 , 49, 47	√
51	Node 50 , 51, 49	√
52	Node 52 , 59, 60	√
53	Node 55 , 54, 53	√
54	Node 55 , 54, 53	√
55	Node 55 , 54, 53	√
56	Node 56 , 54, 57	√
57	Node 57 , 56, 54	√
58	Node 55 , 53, 54	×
62	Node 61 , 60, 63	×
63	Node 63 , 62, 61	√
64	Node 64 , 59, 60	√

From all simulation results done by this research, the method can locate the fault area correctly; the accuracy for this fault location method is about 95 percent which is very high in such a complex network. From fault feature value waveform, not only the fault area can be located correctly, but also the impact on other nodes can be obtained from the feature value. The smaller the value is, the nearer the node is from fault node.

### V. CONCLUSIONS

The proposed fault area location method for distribution network with DG considers about the existence of the nonlinearity of load and grounding resistor. The load model adopts quadric polynomial model; the grounding resistor adopts the experience formula model; the nonlinear equation constructed by nodal voltage equation will be solved out through quasi-Newton algorithm, then the fault area can be located according to the definition of fault feature value. The simulation results suggest the accuracy of the proposed area location method is over 90 percent. The follow-up work is to research on fault precise location method combined with artificial intelligence optimization algorithm.

### ACKNOWLEDGMENT

This paper is sponsored by the National Nature Science Fund Project of China (61271001) and the Fundamental Research Funds for the Central Universities of China under Grant No. 14CX05039A. The authors are grateful for all the reviewers for valuable suggestions to improve the quality of this paper.

### REFERENCES

- [1] Y. Y. Chen, J. Qin, X. Wang, S. Y. Chen, B. B. Zhang, and Yu Yu-Ze, "A survey on fault location for distribution network," *Power System Technology*, vol. 18, pp. 89-93, Sep. 2006.
- [2] S. A. M. Javadian, A. M. Nasrabadi, M. R. Haghifam, and J. Rezvantalab, "Determining fault's type and accurate location in distribution systems with DG using MLP neural networks," in *Proc. International Conference on Clean Electrical Power*, Ischia, 2009, pp. 284-289.
- [3] A. F. Naiem, Y. Hegazy, A. Y. Abdelaziz, and M. A. A. Elsharkaw, "Classification technique for recloser-fuse coordination in distribution systems with distributed generation," *IEEE Transactions on Power Delivery*, vol. 27, pp. 176-185, Jan. 2011.
- [4] Z. Hadi, M. Azah, S. Hussain, and M. Marjan, "Determining exact fault location in a distribution network in presence of DGs using RBF neural networks," in *Proc. IEEE International Conference on Information Reuse and Integration*, Las Vegas, 2011, pp. 434-438.
- [5] Z. J. Kang, A. Tian, and Z. Bai, "A fault area location method in distribution network with DG," *Telkomnika - Indonesian Journal of Electrical Engineering*, vol. 11, pp. 6870-6878, Nov. 2013.
- [6] Y. Y. Feng and Z. J. Kang, "Research on fault location in distributed network with DG based on complex correlation thevenin equivalent and strong tracking filter," in *Proc. Academic Annual Meeting of China Electrotechnical Society*, Weihai, 2013, pp. 196-202.
- [7] M. A. Yahui, "Studies on composite load modeling of distribution network considering distributed generation," M.S. thesis, Hunan University, Hunan, China, 2013.
- [8] V. V. Terzija, R. C. Iric, and H. Nouri, "Improved fault analysis method based on a new arc resistance formula," *IEEE Transactions on Power Delivery*, vol. 26, no. 1, pp. 120-126, Jan. 2011.
- [9] Y. Chen, P. Jiang, Q. L. Wan, and S. Gao, *Power System Analysis*, Beijing: China Power Press, 2005, pp. 16-39.
- [10] F. Chen, "Several methods of the large scale nonlinear equations," M.S. thesis, China University of Mining and Technology, Xuzhou, China, 2014.
- [11] H. J. Zhang, J. Zhao, and H. Luo, "Simultaneous perturbation stochastic approximation algorithm based on quasi-Newton method," *J. Huazhong Univ. of Sci. & Tech. (Natural Science Edition)*, vol. 9, pp. 1-4, Sep. 2014.



**Ruiying Liu** was born in 1990. She received her B.S. degree from China University of Petroleum in 2013. Now she is studying as a second grade postgraduate. Her research field focuses on electrical system design and fault detection and diagnosis.



**Zhongjian Kang** was born in Anyue, China in 1971. He received his bachelor degree from China University of Petroleum in 1993 and received his master degree and doctor degree from Harbin Institute of Technology in 1998 and 2001. Currently, he is a professor in the Department of Electrical Engineering of China University of Petroleum. Prof. Kang's research interests include Power system

analysis and control, Power system fault detection and diagnosis, Oilfield automation equipment development and renewable energy generation control.



**Yanyan Feng** was born in 1989. She received her B.S. degree from China University of Petroleum in 2011 and M.S. degree from China University of Petroleum in 2014. Her research field focuses on electrical system design and fault detection and diagnosis.